# Supplemental Materials

# Magnetocaloric Properties and Microstructures of $HoB_2$ and Nb-Substituted $HoB_2$

Mahboobeh Shahbazi[1,2], Ali Dehghan Manshadi[3], Kiran Shinde[4], Ian Mackinnon[2,5,*]

[1] Centre for Materials Science and School of Chemistry and Physics, Queensland University of Technology,
Brisbane, QLD 4001, Australia; mahboobeh.shahbazi@qut.edu.au
[2] Centre for Clean Energy Technologies and Practices, Queensland University of Technology, Brisbane, QLD 4001, Australia
[3] School of Mechanical and Mining Engineering, The University of Queensland, Brisbane, QLD 4072, Australia; aliuow@gmail.com
[4] Department of Nanotechnology and Advanced Materials Engineering, Sejong University, Seoul 05006, Republic of Korea; yourkirans@gmail.com
[5] School of Earth and Atmospheric Sciences, Queensland University of Technology, Brisbane, QLD 4001, Australia
* Correspondence: ian.mackinnon@qut.edu.au

Table S1: ICP-OES Analysis of trace/minor elements in starting Ho powder

| Analyte | Ho bulk (mg/kg) |
|---|---|
| 11 B | 8.136 |
| 24 Mg | <4.294 |
| 27 Al | 2.129 |
| 40 Ca | 85.221 |
| 47 Ti | <0.672 |
| 55 Mn | 3.56 |
| 56 Fe | 19.005 |
| 60 Ni | 74.696 |
| 63 Cu | 157.951 |
| 89 Y | 20.953 |
| 125 Nb | 49.22 |
| 139 La | 0.517 |
| 140 Ce | 0.339 |
| 141 Pr | 0.105 |
| 146 Nd | 0.616 |
| 147 Sm | 0.541 |
| 157 Gd | 0.129 |
| 159 Tb | 0.129 |
| 163 Dy | 722.425 |
| 166 Er | 536.749 |
| 169 Tm | 51.593 |
| 172 Yb | 0.052 |
| 175 Lu | 25.829 |
| 213 Ta | 3699.515 |
| 214 W | 164.924 |
| **Totals (mg/kg)** | 5624.334 |

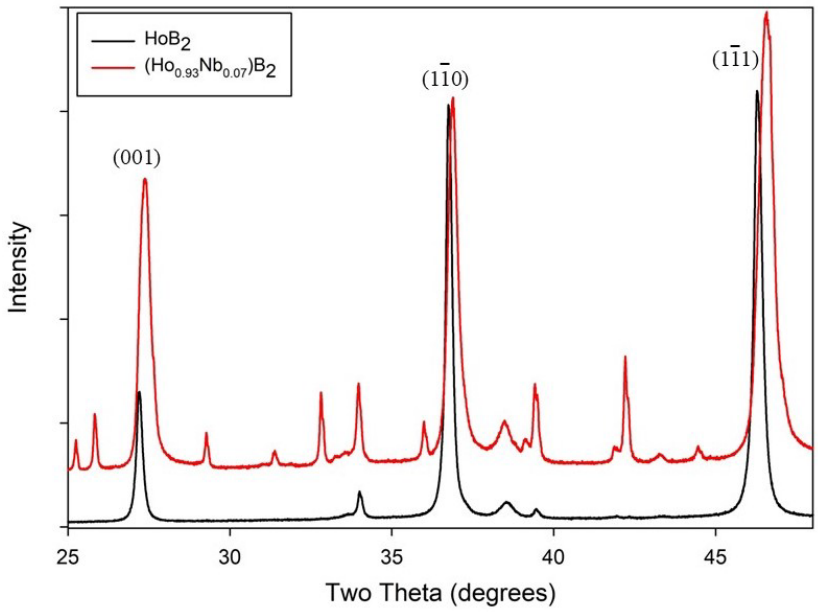



Figure S1: Powder XRD patterns for $25^o < 2\theta < 50^o$ for $HoB_2$ (black) and $Ho_{0.93}Nb_{0.07}B_2$ (red) produced by arc melting as listed in Table 1. Peaks for the $HoB_2$ structure are indexed. Note the shift of peaks for $Ho_{0.93}Nb_{0.07}B_2$ to higher values of $2\theta$ compared to $HoB_2$.

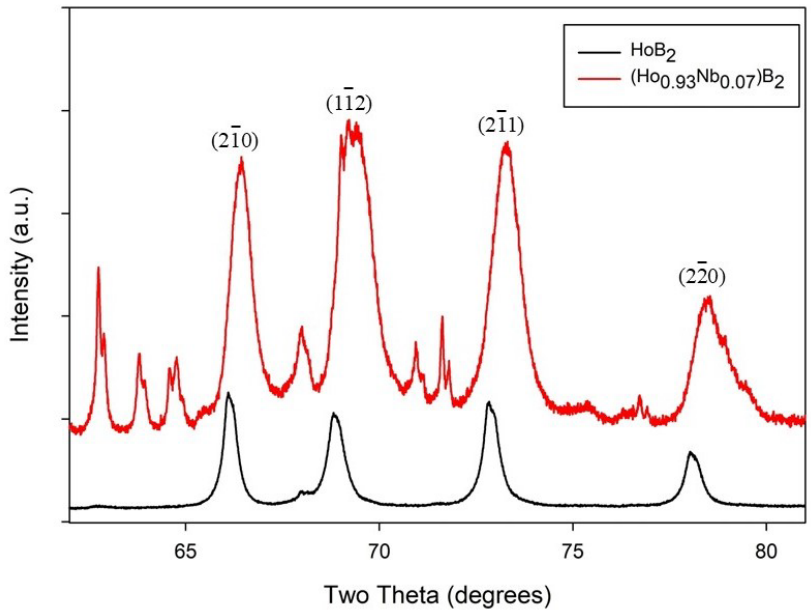



Figure S2: Powder XRD patterns for $60^o < 2\theta < 83^o$ for $HoB_2$ (black) and $Ho_{0.93}Nb_{0.07}B_2$ (red) produced by arc melting as listed in Table 1. Peaks for the $HoB_2$ structure are indexed. Note the broadening of peaks for $Ho_{0.93}Nb_{0.07}B_2$ and shift to higher values of $2\theta$ compared to $HoB_2$.

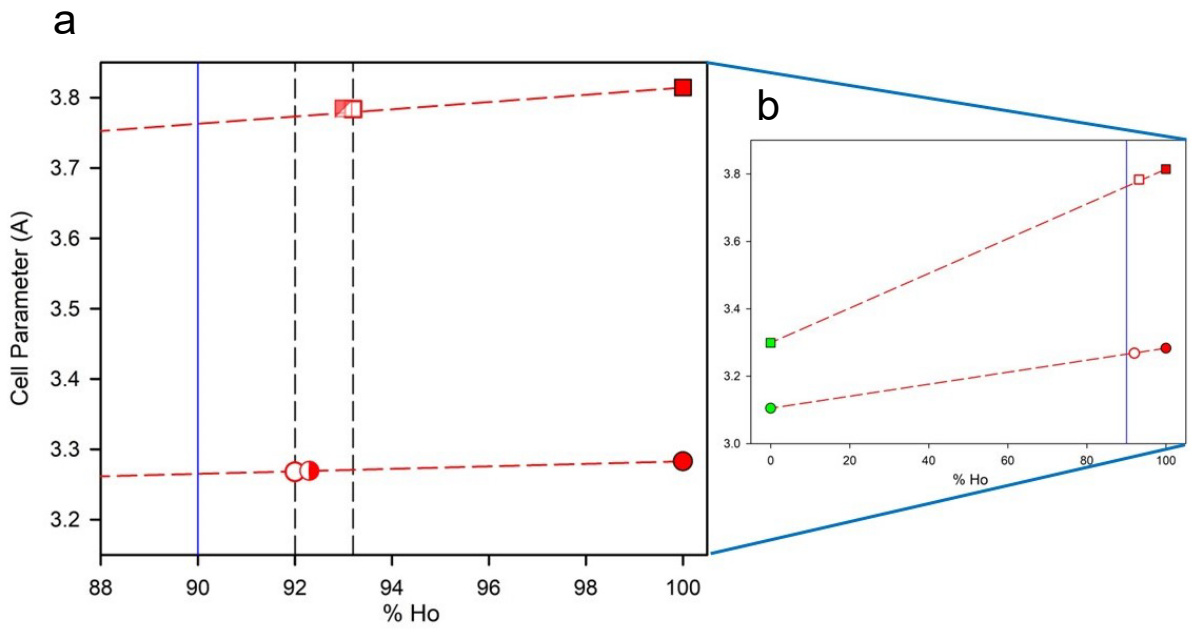



Figure S3: Plot showing unit cell parameters, *a* (filled circles) and *c* (filled squares) for $HoB_2$ (red) and $NbB_2$ (green) in Figure S3(b). The vertical blue line at 90% Ho content is at the nominal substitution of Nb based on initial synthesis mixture listed in Table 1. Open symbols show values for the refined unit cell determined for the $(Ho_{1-x}Nb_x)B_2$ arc melted product. Nb substitution is between 8.0 % (*a* axis) and 6.8 % (*c* axis) defined by the dotted vertical lines in Figure S3(a); half-filled symbols represent values for crystallite size corrections derived from SEM images shown in Figure 2. These crystallite size corrections are within the substitutional range identified in Figure S3(a) (*e.g.* 7.75% and 7.0% Nb, respectively). We conclude from Figure S3 that Nb is soluble in $HoB_2$.